Optothermal Properties of Fibers. VIII. Structure Orientation Study of Annealed Egyptian Polyester Fibers

A. A. HAMZA, I. M. FOUDA, M. A. KABEEL, E. A. SEISA, F. M. EL-SHARKAWY

Physics Department, Faculty of Science, Mansoura University, Mansoura, Egypt

Received 22 March 1996; accepted 5 February 1997

ABSTRACT: A two-beam interferometric method is used to study the change of optical orientation functions and the molecular structure of annealed Egyptian poly(ethylene terephthalate) (PET) fibers. The acoustic method was used for measuring the density. The density results were used to calculate the degree of crystallinity of PET. It was found that annealing causes alignment to the fiber chains in the directions of the fiber axis. This alignment gives an increase in the optical orientation function and decrease in orientation angle. The value of $\Delta\alpha/3\alpha_0$, which depends upon the molecular structure of the polymer, remains constant. The obtained results of the optical and the density clarify that new reorientations occurred due to annealing at different conditions. The changes of the refractive index profile of annealed PET fibers are given. Microinterferograms and curves are given for illustration. © 1997 John Wiley & Sons, Inc. J Appl Polym Sci **65:** 2031–2050, 1997

INTRODUCTION

Several studies have been made of the development of molecular orientation in poly(ethylene terephthalate) (PET) because of its technological importance in the oriented state.[1] PET is a polycrystalline polymer, with a structural order on the molecular and interlamellar levels. The character of this structure varies with the conditions of fabrication.

A polycrystalline polymer is composed of both crystalline and noncrystalline regions. The amount and structural arrangement of these regions within a given sample will depend on how the polymer was fabricated. Since the properties of both the crystalline and noncrystalline region are anisotropic and different from each other, their amount and arrangement will govern the bulk properties of the polymer.[2]

It is known that birefringence is one of the most sensitive indicators of the extent of the anisotropy of properties of polymers and, therefore, the degree of macromolecular orientation. The coefficient of birefringence is often used as a measure of polymer orientation. Structural techniques based on optical birefringence[3–11] were used to measure the degree of the molecular alignment in uniaxially oriented fibers. The birefringence measurement is thus a rapid and powerful tool for the study of morphological characteristics of deformed polycrystalline polymers. Since birefringence is a measure of the total molecular orientation of the two-phase system, its examination in conjunction with other physical measurements (X-ray, density, mechanical loss factor, etc.) yields considerable insight into the characteristic of the bulk polymer.[12] One of the important parameters characterizing the crystalline structure of polymers is the degree of crystallinity, and the density of the polymer has a great influence on the viscoelastic properties of crystalline polymers.[13] Also, it is known that annealing at different conditions leads to a change in the density, crystallinity, mechanical properties, etc.

In this work, the optical orientation function of PET fibers with different annealing conditions was studied to estimate the variation due to the annealing process and, on the other hand, to describe these variations, which may lead to under-

Correspondence to: I. M. Fouda.

 CCC 0021-8995/97/102031-20

standing of the molecular structure to the applied annealing process. A two-beam interferometric method and resonance technique were used to evaluate the orientation and crystallinity parameters.

OVERVIEW

Theoretical Consideration

The mean value of the refractive index of the fiber is calculated from the totally duplicated images of the fiber using the Pluta interference microscope[14,15]; the following expression[16] is used to overcome any irregularity in the fiber cross section:

$$n_a^{\parallel} = n_L + (\lambda/h)\cdot(F^{\parallel}/A) \qquad (1)$$

with an analogous formula for $n_a^{\perp}$, where $n_a^{\parallel}$ and $n_a^{\perp}$ are the mean refractive indices of the fiber for light vibrating parallel and perpendicular to the fiber axis, respectively; $F^{\parallel}$ and $F^{\perp}$ are the area of the fiber enclosed under the fringe shift when using a monochromatic light of wavelength λ. h is the interference fringe spacing in the liquid region; A, the mean cross-sectional area of the fiber; and n_L, the refractive index of the immersion liquid.

The mean birefringence Δn_a of the fiber can be determined from the values of the difference between $n_a^{\parallel}$ and $n_a^{\perp}$, i.e.,

$$\Delta n_a = n_a^{\parallel} - n_a^{\perp}$$

Considering the nonduplicated image of the fiber, using a Pluta polarizing interference microscope, the birefringence can be calculated from the formula

$$\Delta n_a = \frac{\Delta F \lambda}{hA} \qquad (2)$$

where ΔF is the area enclosed under the fringe shift using a nonduplicated image of the fiber.

The optical results of the refractive indices for light vibrating in the directions parallel and perpendicular to the fiber axis were utilized in calculating the following parameters: the polarizabilities per unit volume, the isotropic polarizability, the isotropic refractive index, the optical orientation factor, the orientation angle, and the specific volume of annealed polyester fiber at different temperatures (80–190 ± 1°C) for different times ($P^{\parallel}$, $P^{\perp}$, P_0, n_{iso}, f_θ, V) according to the following relations[17–19]:

$$(n_{\parallel}^2 - 1)/(n_{\parallel}^2 + 2) = (4/3)\pi P^{\parallel} \qquad (3)$$

where $P^{\parallel}$ is the polarizability per unit volume and an analogous equation in the perpendicular direction and

$$P_{\text{iso}} = (P^{\parallel} + 2P^{\perp})/3 \qquad (4)$$

where P_{iso} is the isotropic polarizability. The isotropic refractive index n_{iso} (ref. 20) is

$$n_{\text{iso}} = (n_a^{\parallel} + 2n_a^{\perp})/3 \qquad (5)$$

which is related to the following relation to obtain the specific volume:

$$(n_{\text{iso}} - 1)V = K \qquad (6)$$

Experimental verification of the above relation shows that the constant (K) of relation (6) lies within 0.40–0.46.

The optical orientation function can be found using Hermans' equation[21]:

$$(\text{Opt. Ori. Fun.})f_\theta = \Delta n_a/\Delta n_{\max} \qquad (7)$$

where $\Delta n_{\max}$ is the maximum birefringence for fully oriented fiber and Δn_a is the birefringence of the fiber under investigation. f_θ values are in the range $+1$, 0, $-\frac{1}{2}$ according to the state of orientation: perfect, random or perpendicular to the fiber axis, respectively. The value of $\Delta n_{\max}$ was previously determined to be 0.24.[22]

Also, the optical orientation angle can be found by using the following equation:

$$f_\theta = 1 - (3/2)\sin^2_\theta \qquad (8)$$

where θ is the angle between the axis of polymer unit and the fiber axis. The average value of the optical orientation function, $\langle P_2(\theta)\rangle$, due to Ward,[23,24] is given by

$$\langle P_2(\theta)\rangle = \Delta n_a/\Delta n_{\max} \qquad (9)$$

which is the same function named by Hermans.[21] $\langle P_{21}(\theta)\rangle$ is related to the polarizability per unit volume[25] as follows:

$$\{\Phi^{\parallel} - \Phi^{\perp}/\Phi^{\parallel} + 2\Phi^{\perp}\} = P_2(\theta_m)\langle P_2(\theta)\rangle \qquad (10)$$

where $\Phi^{\parallel}$ and $\Phi^{\perp}$ are the polarizabilities directions parallel and perpendicular to the fiber axis, respectively, where

$$P_2(\theta_m) = \tfrac{1}{2}(3\cos^2\theta_m - 1) = \text{constant quantity}$$

Also, eq. (10) can be written in the form

$$\{\Phi^{\parallel} - \Phi^{\perp}/\Phi^{\parallel} + 2\Phi^{\perp}\} = [\Delta\alpha/3\alpha_0]\langle P_2(\theta)\rangle \quad (11)$$

where $\Delta\alpha$ is the difference between $\alpha^{\parallel}$ and $\alpha^{\perp}$, which are the electric polarizability of one molecule when using monochromatic light vibrating parallel and perpendicular to the fiber axis, respectively. The quantity $(\Delta\alpha/3\alpha_0)$ depends on the molecular structure and is nearly constant for a given polymer.[6] The values of $\Phi^{\parallel}$ and $\Phi^{\perp}$ can be determined from eq. (3) due to (cf. Stein and Wilkes[26])

$$[n_{\parallel}^2 - 1/n_{\parallel}^2 + 2] = \Phi^{\parallel} \quad (12)$$

In a recent approach to the continuum theory of birefringence of the oriented polymer,[22] it was found that the value of f_θ, i.e.,

$$f_\theta = [n_1^2 n_2^2/n_{\parallel}^2 n_{\perp}^2]\cdot[n_{\parallel} + n_{\perp}/n_1 + n_2] \times \Delta n_a/\Delta n_{\max} \quad (13)$$

which is slightly different from the original simple expression of the degree of orientation in eq. (7) used by Hermans and Platzek[27] and Kratky,[28] can be given by the following equation:

$$f_\theta = (1 + a)f_\Delta - af_\Delta \quad (14)$$

$$(1 + a) = 2n_1^2 n_2^2/n_\nu^2(n_1 + n_2)$$

$$f_\Delta = \Delta n_a/\Delta n_{\max} \quad (15)$$

where n_1, n_2, and n_ν were given in ref. 22 and $n_\nu = n_{\text{iso}}$. From eq. (15), the constant a was calculated and found to be 0.880. Also, the specific refractivity of the isotropic dielectric can be determined by the following equation[21]:

$$[n_{\text{iso}}^2 - 1/n_{\text{iso}}^2 + 2] = \varepsilon\rho \quad (16)$$

where ρ is the density, and ε, the specific refractivity of the isotropic dielectric. P_0, n_{iso}, V, ε, and $\Delta\alpha/3\alpha_0$ for PET can be calculated and are given in Table I.

EXPERIMENTAL

Density Measurements

For the measurement of the fiber density, the measuring system was discussed in detail elsewhere.[29–31] From the following equation,[32]

$$f_0 = (p/2\ell)(T/m)^{(1/2)} \quad (17)$$

the mass per unit length m can be calculated, where f_0 is the resonance frequency; p, the number of resonance modes within the string's length ℓ, and T, the tensional force. From the obtained value of the mass per unit length m, one easily calculate the density, ρ, of the fiber material from the relation

$$\rho = m/(\pi r^2) \quad (18)$$

where r is the radius of the cylindrical fiber.

The following measuring conditions were satisfied for high accuracy:

1. The fiber diameter is sufficiently narrow in such a way that the shift in the resonance frequency due to air damping could be neglected.
2. The length of the fiber should be selected in such a way that the resonance frequency is located within a frequency region completely free from any other resonance peaks due to natural frequencies of the system. This avoids the effect of resonance coupling.
3. The loading mass should be sufficiently small to avoid any serious structural variations due to the mechanical creep in the same sample.

Crystallinity Determination

The degree of crystallinity was determined by the relation[33]

$$\chi = (\rho - \rho_a)/(\rho_c - \rho_a) \quad (19)$$

where $\rho_c = 1.457$ g/cm^3, $\rho_a = 1.336$ g/cm^3 (refs. 33–35), and ρ is the density measurement. The values of ρ, K, and χ for PET were calculated and are given in Table II.

Table I P_0, n_{iso}, V, ε, and $\Delta\alpha/3\alpha_0$ Values Calculated for PET

Annealing Temperature (°C)	P_{iso}	n_{iso}	V	$\varepsilon^{\parallel}$	$\varepsilon^{\perp}$	ε_{iso}	$\frac{\Delta\alpha}{3\alpha_0}$
			(a) At Constant Time of 1 h				
Unannealed	0.0798	1.584	0.7257	0.2503	0.2389	0.2427	0.1035
80	0.08022	1.587	0.7323	0.2527	0.2429	0.2462	0.1035
100	0.08177	1.602	0.7182	0.2658	0.2362	0.2463	0.1035
120	0.08181	1.602	0.7199	0.2671	0.2366	0.2470	0.1035
140	0.08227	1.607	0.7100	0.2684	0.2330	0.2451	0.1035
160	0.08175	1.602	0.7188	0.2724	0.2332	0.2467	0.1035
170	0.08278	1.612	0.7127	0.2731	0.2343	0.2476	0.1035
180	0.08278	1.612	0.7093	0.2749	0.2316	0.2466	0.1035
190	0.08033	1.589	0.7352	0.2605	0.2410	0.2476	0.1035
			(b) At Constant Time of 2 h				
Unannealed	0.0798	1.584	0.7257	0.2503	0.2389	0.2427	0.1035
80	0.0802	1.588	0.7231	0.2463	0.2416	0.2432	0.1035
100	0.0820	1.604	0.7121	0.2628	0.2355	0.2448	0.1035
120	0.0816	1.601	0.7230	0.2689	0.2365	0.2476	0.1035
140	0.0817	1.601	0.7229	0.2707	0.2358	0.2478	0.1035
160	0.0825	1.609	0.7118	0.2712	0.2337	0.2465	0.1035
170	0.0823	1.607	0.7143	0.2712	0.2339	0.2467	0.1035
180	0.0826	1.610	0.7120	0.2729	0.2329	0.2467	0.1035
190	0.0828	1.612	0.7481	0.2898	0.2442	0.2599	0.1035
			(c) At Constant Time of 4 h				
Unannealed	0.0798	1.584	0.7257	0.2503	0.2389	0.2427	0.1035
80	0.0798	1.583	0.7342	0.2506	0.2428	0.2454	0.1035
100	0.0820	1.604	0.7178	0.2639	0.2381	0.2469	0.1035
120	0.0821	1.605	0.7145	0.2674	0.2352	0.2462	0.1035
140	0.0819	1.604	0.7078	0.2657	0.2317	0.2434	0.1035
160	0.0814	1.599	0.7216	0.2715	0.2333	0.2464	0.1035
170	0.0818	1.602	0.7117	0.2689	0.2314	0.2443	0.1035
180	0.0820	1.605	0.7167	0.2738	0.2326	0.2467	0.1035
190	0.0829	1.614	0.7136	0.2806	0.2317	0.2487	0.1035
			(d) At Constant Time of 5 h				
Unannealed	0.0798	1.5835	0.7257	0.2503	0.2389	0.2427	0.1035
80	0.0800	1.5853	0.7331	0.2522	0.2426	0.2458	0.1035
100	0.0819	1.6027	0.7198	0.2626	0.2392	0.2472	0.1035
120	0.0820	1.6043	0.7183	0.2699	0.2353	0.2472	0.1035
140	0.0817	1.6013	0.7235	0.2734	0.2346	0.2480	0.1035
160	0.0824	1.6083	0.7125	0.2732	0.2324	0.2465	0.1035
170	0.0823	1.6070	0.7166	0.2751	0.2329	0.2475	0.1035
180	0.0829	1.6130	0.7089	0.2779	0.2302	0.2468	0.1035
190	0.0831	1.6153	0.7083	0.2789	0.2305	0.2473	0.1035

(continued)

Refractive Index Profile of Annealed Fiber at Different Temperatures for Different Times

In the case of two-beam interference fringes crossing a cylindrical multilayer fiber, immersed in a liquid of refractive index n_L, with m layers of refractive indices $n_1 n_2, \ldots, n_m$, where n_1 is the index of the outer layer and n_m is the index of the inner layer (core), one can derive the mathematical formula[36]

Table I (*Continued from the previous page*)

Annealing Temperature (°C)	P_{iso}	n_{iso}	V	$\varepsilon^{\parallel}$	$\varepsilon^{\perp}$	ε_{iso}	$\frac{\Delta\alpha}{3\alpha_0}$
			(e) At Constant Time of 7 h				
Unannealed	0.0798	1.584	0.7257	0.2503	0.2389	0.2427	0.1035
80	0.0794	1.579	0.7418	0.2481	0.2460	0.2467	0.1035
100	0.0823	1.607	0.7064	0.2597	0.2357	0.2438	0.1035
120	0.0820	1.604	0.7164	0.2678	0.2363	0.2471	0.1035
140	0.0822	1.606	0.7188	0.2706	0.2362	0.2480	0.1035
160	0.0824	1.608	0.7054	0.2682	0.2314	0.2440	0.1035
170	0.0829	1.613	0.7054	0.2716	0.2316	0.2454	0.1035
180	0.0828	1.612	0.7058	0.2736	0.2305	0.2454	0.1035
190	0.0830	1.614	0.7013	0.2737	0.2292	0.2446	0.1035
			(f) At Constant Time of 10 h				
Unannealed	0.0798	1.584	0.7256	0.2503	0.2389	0.2427	0.1035
80	0.0796	1.586	0.7230	0.2463	0.2416	0.2432	0.1035
100	0.0813	1.604	0.7121	0.2628	0.2355	0.2448	0.1035
120	0.0821	1.601	0.7230	0.2689	0.2365	0.2476	0.1035
140	0.0822	1.601	0.7229	0.2707	0.2358	0.2478	0.1035
160	0.0824	1.609	0.7117	0.2712	0.2337	0.2465	0.1035
170	0.0827	1.607	0.7143	0.2712	0.2339	0.2467	0.1035
180	0.0830	1.610	0.7119	0.2729	0.2329	0.2467	0.1035
190	—	—	—	—	—	—	0.1035

$$(\lambda/2h)d_m = \sum_{q=1}^{m} (n_q - n_{q-1})(r_q^2 - r_{m+1}^2)^{1/2}, \qquad q = 1, 2, \cdots m$$

where the fringe shift d_m is related to the value of radii r_{m+1} (at the boundaries of the different layers of the fiber) $n_{q-1} = n_L$, where $q = 1$, n_L is the immersion liquid, λ is the wavelength of monochromatic light, and h is the interfringe spacing. Also, a refractive index profile can be calculated for any circular fiber.

EXPERIMENTAL PROCEDURE AND RESULTS

Sample Preparation

Annealing

The polyester fibers were provided by Kafr EL-Dawar (Egyptian factor). Each fiber was a bundle of ca. 30 filaments. As received, the fibers had a diameter of 26.5 μm, a density of 1.378, and a birefringence number of 0.037, and the initial crystallinity was 34.7% and its orientation function was calculated[37] to be 17.048×10^{-2}.

The polyester fibers were distributed in a cocoon form on a glass rod with free ends which were then heated in an electric oven whose temperature was adjusted to different temperatures (80–190 ± 1°C). Hence, the samples were annealed for the annealing times of 1–10 h, then left to cool at room temperature, 28 ± 1°C.

Optical Microscopy

Plate 1 shows the cross section of polyester fibers seen by high-power optical microscopy. It is clear that polyester fibers have a regular circular cross section.

Double-Beam Inteferometry

The totally duplicated image of the fiber obtained with a Pluta polarizing interference microscope[14,15] was used to calculate the mean refractive indices $n_a^{\parallel}$ and $n_a^{\perp}$ and the birefringence Δn_a of the polyester fibers.

Plate 2 shows a microinterferogram of totally duplicated images of unannealed polyester fiber using the Pluta microscope with a monochromatic light of wavelength 546 nm. The refractive index

Table II ρ, K, and χ Values Calculated for PET

Annealing Temperature (°C)	$n_a^{\parallel}$	$n_a^{\perp}$	$n_{iso} - 1$	ρ	K	$\chi \times 10^{-2}$
			(a) At Constant Time of 1 h			
Unannealed	1.606	1.572	0.5835	1.3780	0.4234	34.71
80	1.606	1.578	0.5872	1.3655	0.4030	24.38
100	1.662	1.572	0.6019	1.3924	0.4032	46.61
120	1.664	1.571	0.6023	1.3891	0.4034	43.88
140	1.680	1.570	0.6068	1.4085	0.4030	59.92
160	1.682	1.562	0.6022	1.3912	0.4033	45.62
170	1.692	1.571	0.6116	1.4032	0.4036	55.54
180	1.703	1.567	0.6120	1.4099	0.4034	61.07
190	1.627	1.569	0.5885	1.3601	0.4033	19.92
			(b) At Constant Time of 2 h			
Unannealed	1.606	1.572	0.5835	1.3780	0.4234	34.71
80	1.597	1.583	0.5875	1.3827	0.4249	39.75
100	1.660	1.576	0.6036	1.4043	0.4298	56.45
120	1.666	1.568	0.6006	1.3831	0.4343	38.93
140	1.672	1.566	0.6013	1.3833	0.4347	39.09
160	1.687	1.570	0.6092	1.4049	0.4336	56.94
170	1.684	1.569	0.6070	1.3999	0.4336	52.81
180	1.693	1.568	0.6096	1.4046	0.4340	56.69
190	1.702	1.567	0.6117	1.4211	0.4576	70.33
			(c) At Constant Time of 4 h			
Unannealed	1.606	1.572	0.5835	1.3780	0.4234	34.71
80	1.598	1.575	0.5830	1.3620	0.4280	21.49
100	1.657	1.578	0.6039	1.3931	0.4335	47.19
120	1.671	1.572	0.6053	1.3995	0.4325	52.48
140	1.674	1.568	0.6037	1.4129	0.4273	63.55
160	1.676	1.560	0.5986	1.3859	0.4320	41.24
170	1.680	1.564	0.6024	1.4050	0.4287	57.03
180	1.690	1.563	0.6048	1.3952	0.4335	48.93
190	1.716	1.563	0.6138	1.4014	0.4380	54.05
			(d) At Constant Time of 5 h			
Unannealed	1.606	1.572	0.5835	1.3780	0.4234	34.71
80	1.604	1.577	0.5853	1.3640	0.4291	23.14
100	1.650	1.579	0.6027	1.3892	0.4338	43.97
120	1.675	1.569	0.6043	1.3921	0.4341	46.36
140	1.680	1.562	0.6013	1.3821	0.4351	38.10
160	1.693	1.566	0.6083	1.4036	0.4334	55.87
170	1.694	1.535	0.6073	1.3956	0.4352	49.26
180	1.713	1.563	0.6130	1.4106	0.4346	61.65
190	1.717	1.565	0.6153	1.4119	0.4358	62.73

(continued)

of the immersion liquid was 1.6035 at 18°C (in parallel and perpendicular).

Plates 3 and 4 are microinterferograms of the totally duplicated images in parallel and perpendicular directions, respectively, of polyester fiber samples annealed at different temperatures (80–190 ± 1°C) and time intervals of 7 and 10 h. A monochromatic light of wavelength 546 nm was used. In Plates 3 and 4, the immersion liquid was selected to allow the fringe shift to be small

Table II (*Continued from the previous page*)

Annealing Temperature (°C)	$n_a^{\parallel}$	$n_a^{\perp}$	$n_{iso} - 1$	ρ	K	$\chi \times 10^{-2}$
			(e) At Constant Time of 7 h			
Unannealed	1.606	1.572	0.5835	1.3780	0.4234	34.71
80	1.584	1.577	0.5794	1.3572	0.4269	18.50
100	1.657	1.582	0.6067	1.4157	0.4286	65.87
120	1.668	1.572	0.6038	1.3917	0.4339	60.33
140	1.677	1.571	0.6063	1.3913	0.4358	45.70
160	1.686	1.570	0.6084	1.4177	0.4291	67.52
170	1.697	1.570	0.6125	1.4177	0.4320	67.52
180	1.703	1.567	0.6122	1.4168	0.4321	66.78
190	1.709	1.567	0.6144	1.4259	0.4309	74.30
			(f) At Constant Time of 10 h			
Unannealed	1.606	1.572	0.5835	1.3780	0.4234	34.71
80	1.586	1.577	0.5817	1.3501	0.4309	11.65
100	1.646	1.571	0.5970	1.3758	0.4340	32.89
120	1.672	1.571	0.6053	1.3951	0.4339	48.84
140	1.682	1.570	0.6063	1.3917	0.4357	46.03
160	1.689	1.562	0.6079	1.3936	0.4362	47.60
170	1.694	1.571	0.6106	1.4033	0.4351	55.62
180	1.711	1.566	0.6145	1.4132	0.4348	63.80
190	—	—	—	—	—	—

(within one to two orders of interference) and to determine accurately the point of connection of the fringe in the liquid and fiber regions. Plates 3 and 4 also show that the fringe shift increases as the temperature of annealing increases. The refractive indexes of the immersion liquid were 1.658 and 1.569 at 18°C in parallel and perpendicular directions, respectively. Using these interferograms and eq. (1), the mean refractive index of the parallel and perpendicular directions at different annealing intervals and constant annealing temperature was calculated.

Figure 1 shows the variation of $n_a^{\parallel}$ and $n_a^{\perp}$ of the annealed polyester fibers by increasing the annealing temperature (annealing times are 1, 2, 4, 5, 7, and 10 h) as obtained using a Pluta double-beam interference microscope. It is clear that increase in the temperature of annealing increases the orientation of the molecules in the parallel direction. The process of axial orientation increases crystallinity by both orienting the molecules and bringing them closer together, enabling crystallites to form from formerly amorphous regions. It is clear that $n_a^{\perp}$ increased with the temperature of annealing and then decreased slowly and then levels off. This behavior is attributed to disorientation of the mobility of molecules in the perpendicular direction.

Figure 2 shows the variation of Δn_a with the temperature of annealing (annealing times are 1, 2, 4, 5, 7, and 10 h). It is clear that Δn_a increases due to annealing and this means an increase in orientation due to the thermal treatment. The ori-

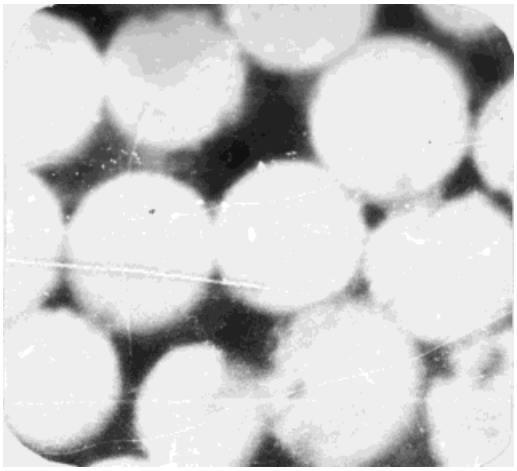

Plate 1 The cross-sectional area of the unannealed PET fiber.

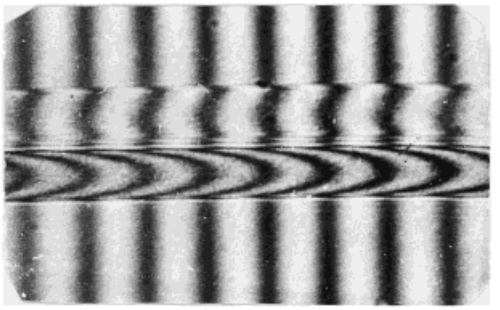

a)

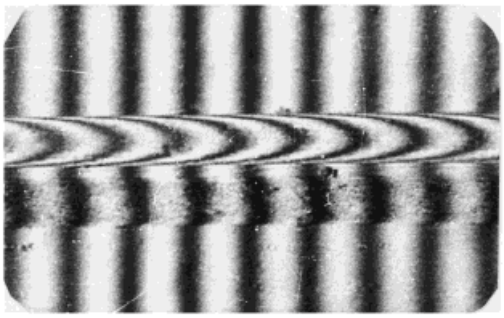

b)

Plate 2 (a, b) Microinterferograms of the duplicated image of polyester (PET) fiber unannealed in parallel and perpendicular directions. A monochromatic light of $\lambda = 546$ nm was used.

entation was attributed to that molecular arrangement in both crystalline and amorphous regions had occurred.

Figure 3 shows the variation of the crystallinity of polyester fibers due to changing annealing temperature for different times periods. Figure 4 shows the variation between the crystallinity and the density of the polyester fibers due to changing annealing for different time periods. Figure 5 shows the relationship between the optical orientation function (f_θ) from eq. (13) of polyester fibers from a duplicated image as a function of annealing temperature (°C).

These results indicate that the annealing of PET fibers effect changes in the overall orientation and the alignment of polymeric chains in parallel and perpendicular directions.[38] So, all the obtained results reported structural changes at a temperature near the T_g (80°C) which was associated with the amorphous nature of PET.

It is important to note that the values of T_g depend on the experimental time scale and the means of measurement. Values of T_g reported in the literature for any particular polymer may vary over a 10–15°C range. For most practical purposes, this variation will not be important.[39] In fact, the characterization and understanding of crystallization in fibrous materials is a long-standing goal in polymer science.[40] The state of the noncrystalline material depends strongly on the temperature of crystallization and the thermal treatment.[41]

So, many studies have been done recently on the kinetics of strain-induced crystallization of PET. However, these works only dealt with the rate of induced crystallization during the annealing of oriented amorphous samples. The initial orientation of the material and the annealing temperature are the two parameters which control the kinetics of strain-induced crystallization.[42] Hence, the present work needs further study, which was not the aim of this article and which will be done in future studies.

Figure 6 shows the angle of orientation as a function of annealing temperatures at different times (1, 2, 4, 5, 7, 10 h). Figure 7 shows the relationship between the optical orientation function $\langle P_2(\theta)\rangle$ and the value $(\Phi^{\parallel} - \Phi^{\perp})/(\Phi^{\parallel} + 2\Phi^{\perp})$. It gives a straight line. The slope of this straight line gives the constant $(\Delta\alpha/3\alpha_0)$ for PET fibers which was found to be 0.103496. Using the value of $\Delta n_{\max} = 0.24$ for PET fibers by de Vries,[20] the values of $\langle P_2(\theta)\rangle$, $(\Phi^{\parallel} - \Phi^{\perp})/(\Phi^{\parallel} + 2\Phi^{\perp})$, and $(\Delta\alpha/3\alpha_0)$ for PET can be calculated.

Figure 8 gives the refractive index profile ($n^{\parallel}$, $n^{\perp}$, and Δn) of polyester fibers with different annealing times. These figures show the change of refractive indices and birefringence across the fiber diameter with annealing times. These curves are indicative of the structure variations due to different annealing conditions.

DISCUSSION

To explain the different variations obtained (Fig. 3), it was essential to take the following assumptions into account[29]: When a polymer is annealed, its structural behavior is altered due to the accumulation of several structural processes. These may be summarized as (a) disorientation, (b) recrystallization by nucleation, (c) recrystallization by growth, (d) shrinkage, and (e) crystal decomposition. These processes are natural responses to both annealing temperature and time.[12,13,41,42] So, summarizing the results of our structure studies, we may develop the following conception about the effect of different annealing conditions on the structure of PET: Two explanations have

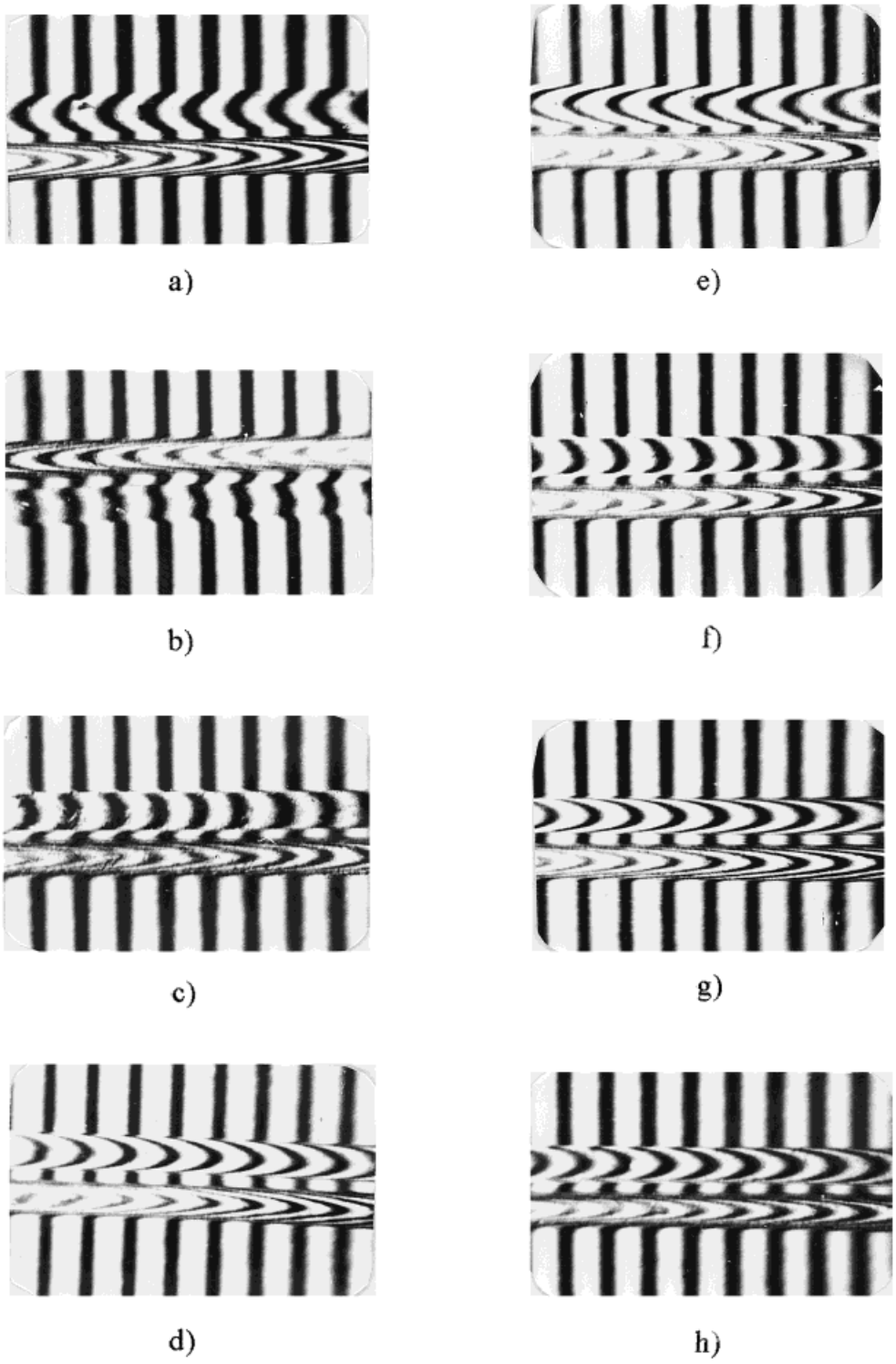

Plate 3 (a–h) Microinterferograms of the totally duplicated image of polyester fiber which was annealed at different temperatures (80–190 ± 1°C) at constant times (7 and 10 h) in parallel and perpendicular directions, respectively. A monochromatic light of $\lambda = 546$ nm was used.

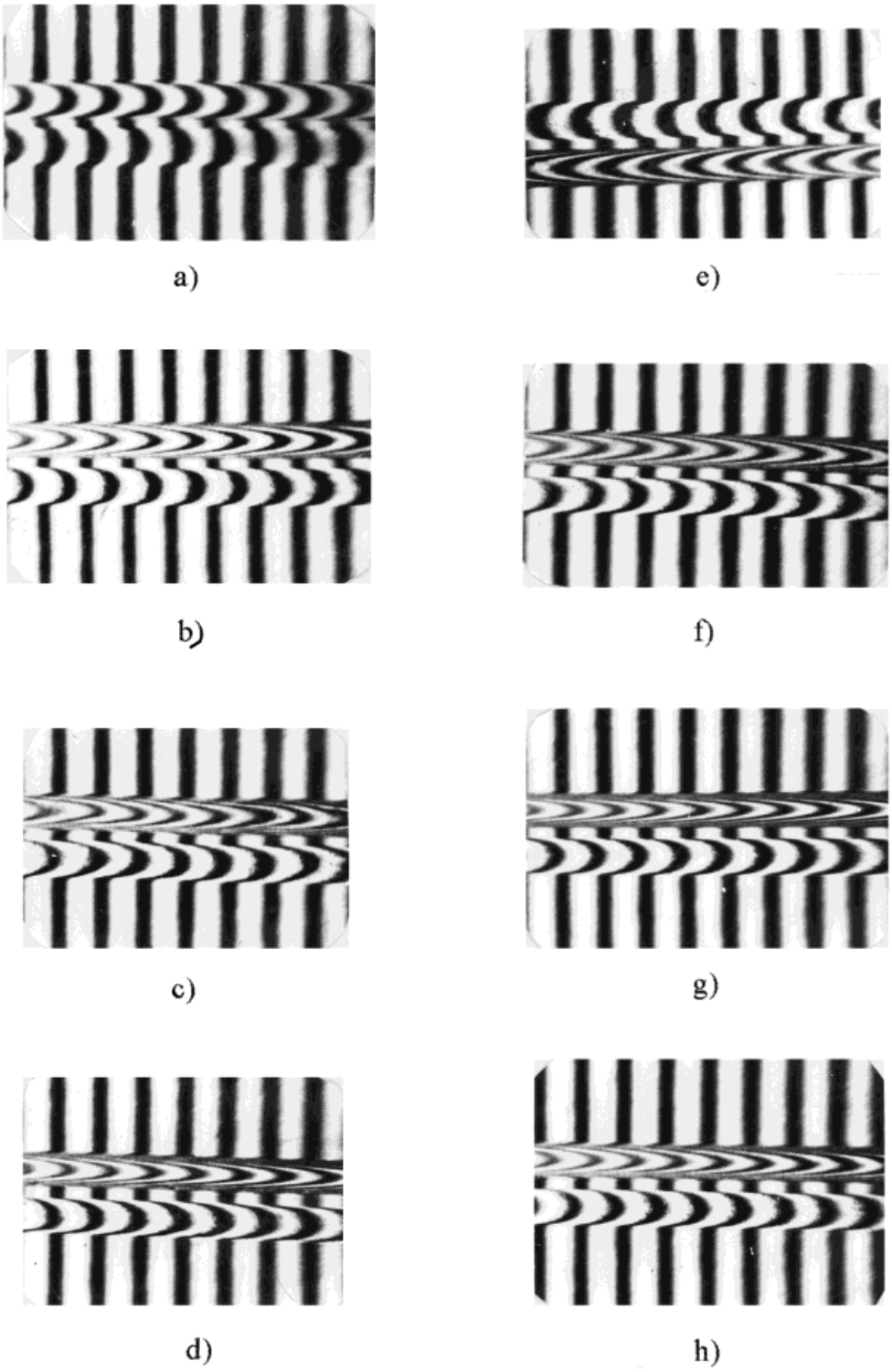

Plate 4 (a–h) Microinterferograms of the totally duplicated image of polyester fiber which was annealed at different temperatures (80–190 ± 1°C) at constant times (7 and 10 h) in parallel and perpendicular directions, respectively. A monochromatic light of $\lambda = 546$ nm was used.

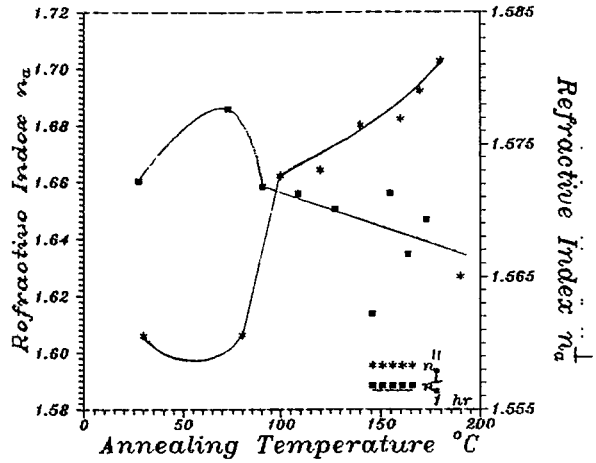

Figure (1-a)

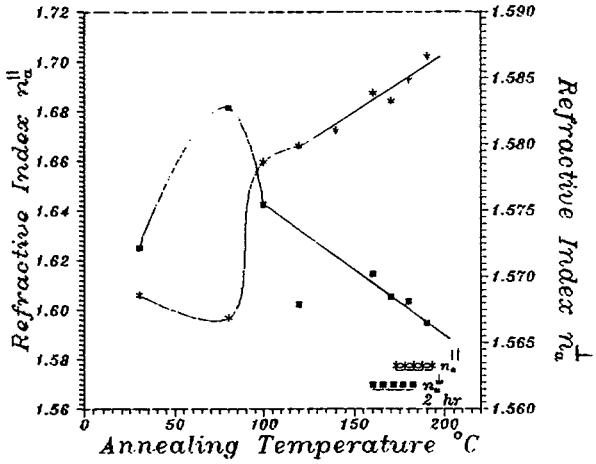

Figure (1-b)

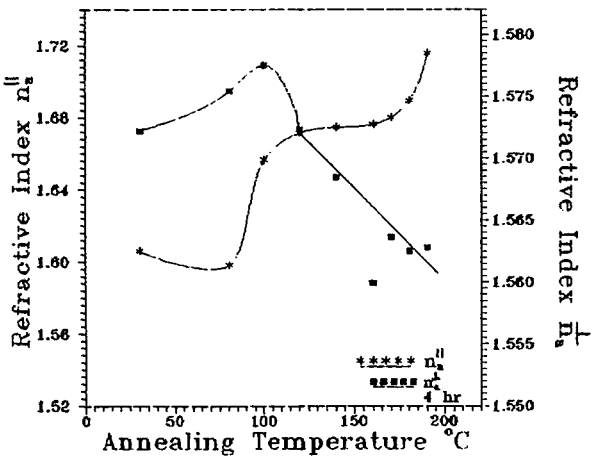

Figure (1-c)

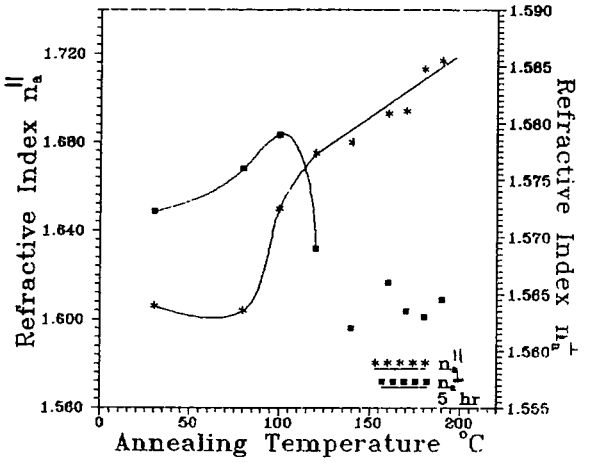

Figure (1-d)

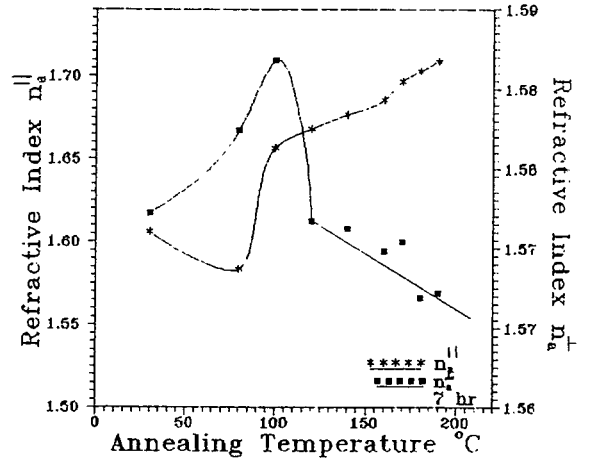

Figure (1-e)

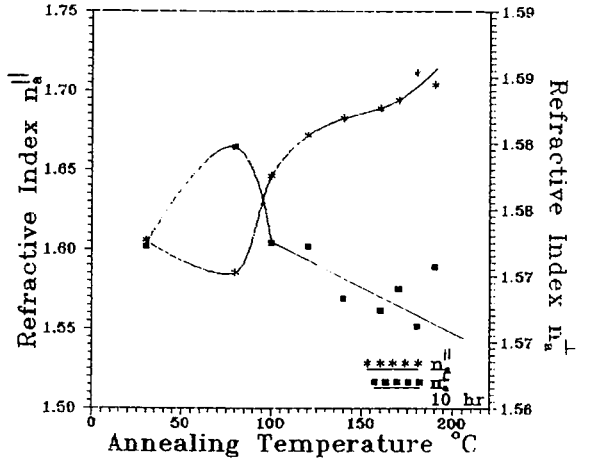

Figure (1-f)

Figure 1 (a–f) Relation between annealed temperatures and refractive index for light-vibrating in parallel and perpendicular directions to the fiber axis $n_a^{\parallel}$ and $n_a^{\perp}$ of polyester fiber at different times (1, 2, 4, 5, 7, and 10 h).

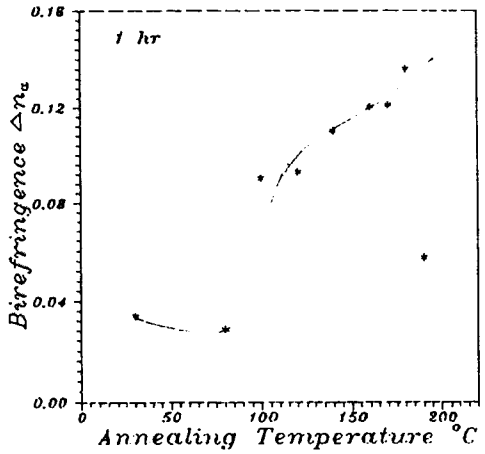

Figure (2-a)

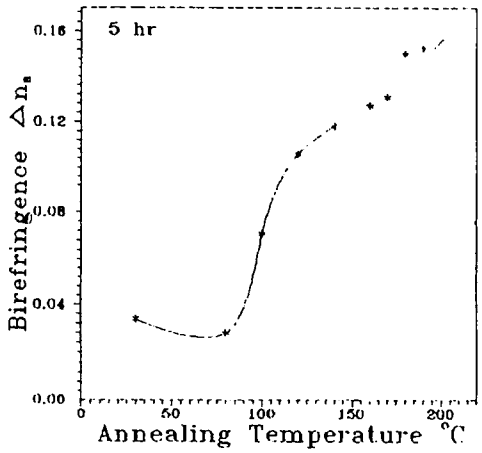

Figure (2-d)

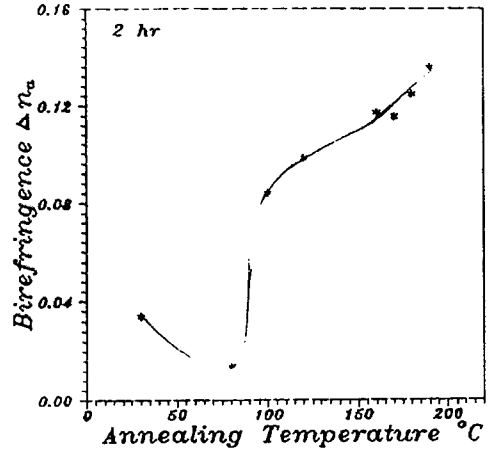

Figure (2-b)

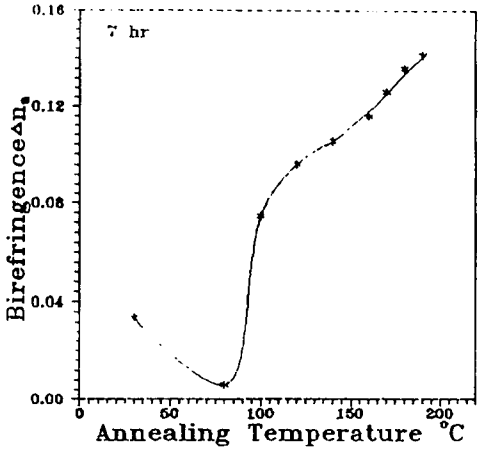

Figure (2-e)

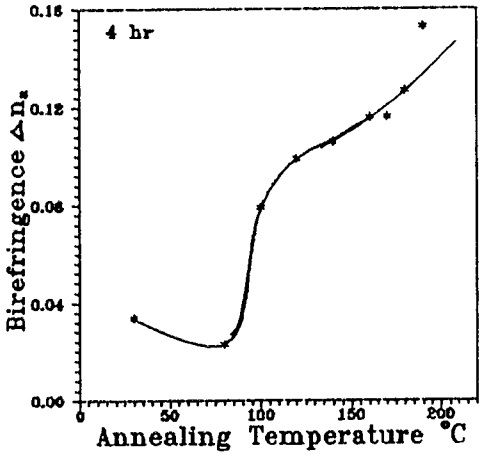

Figure (2-c)

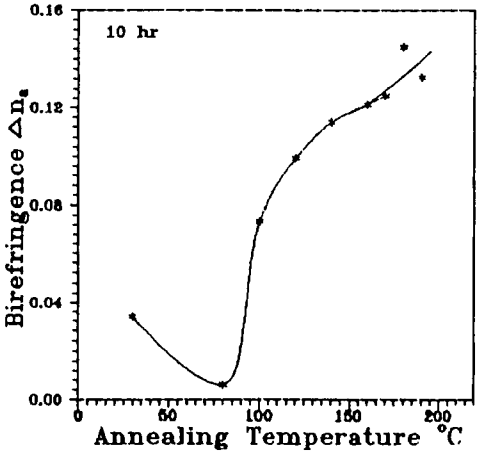

Figure (2-f)

Figure 2 (a–f) Relation between annealed temperature and birefringence of polyester fiber at different times (1, 2, 4, 5, 7, and 10 h).

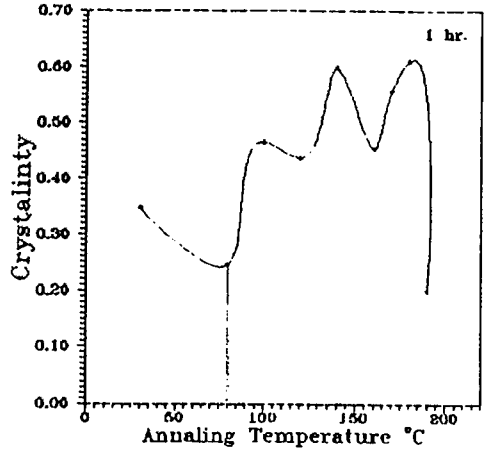

Figure(3-a)

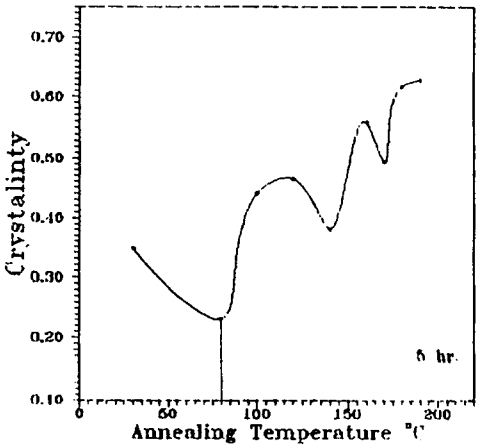

Figure (3-d)

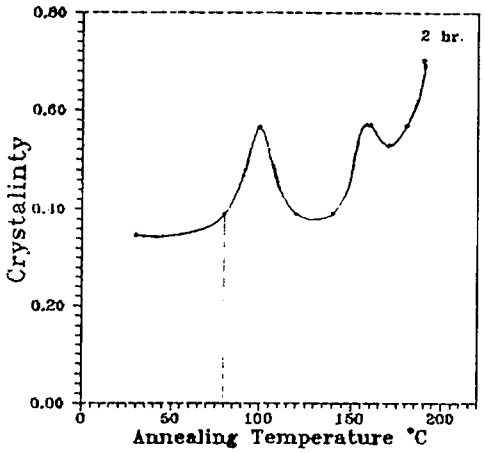

Figure (3-b)

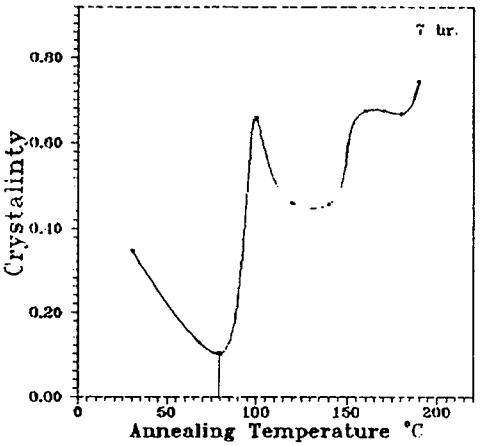

Figure (3-e)

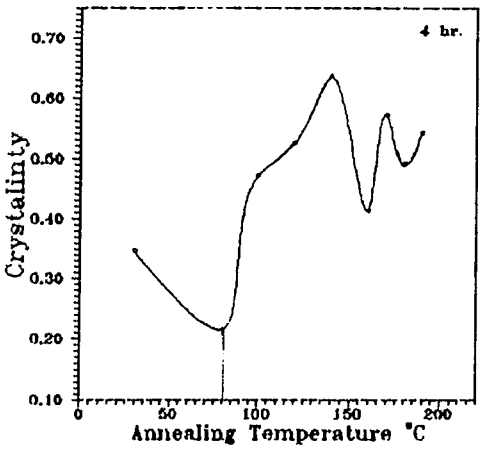

Figure (3-c)

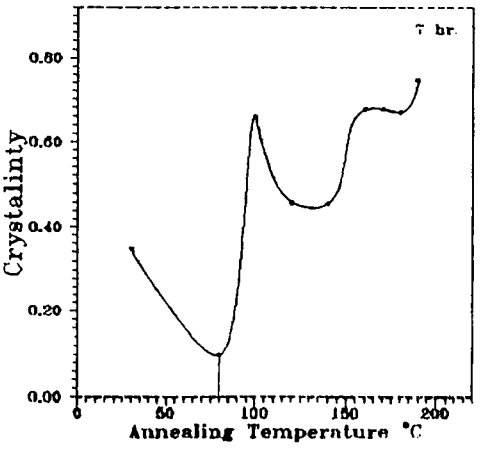

Figure (3-f)

Figure 3 (a–f) Relation between annealed temperature and the crystallinity of polyester fiber at different times (1, 2, 4, 5, 7, and 10 h).

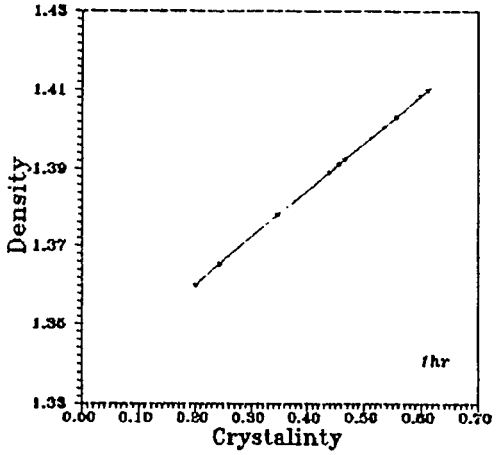

Figure (4--a)

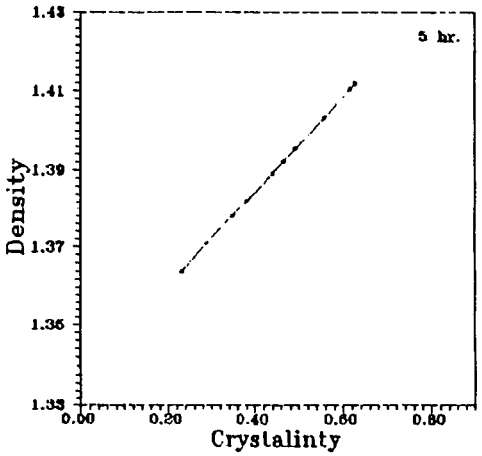

Figure(4-d)

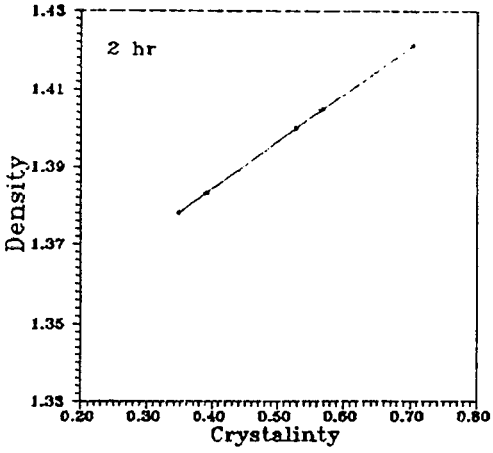

Figure (4-b)

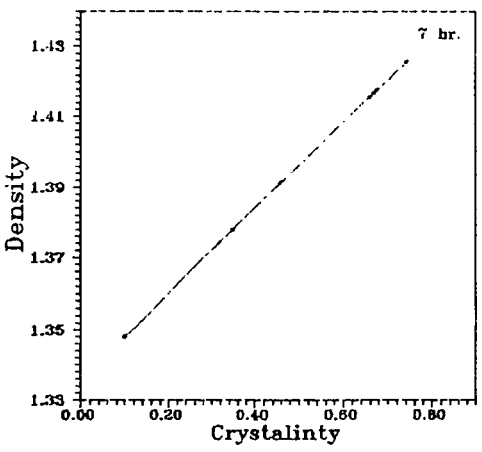

Figure (4-e)

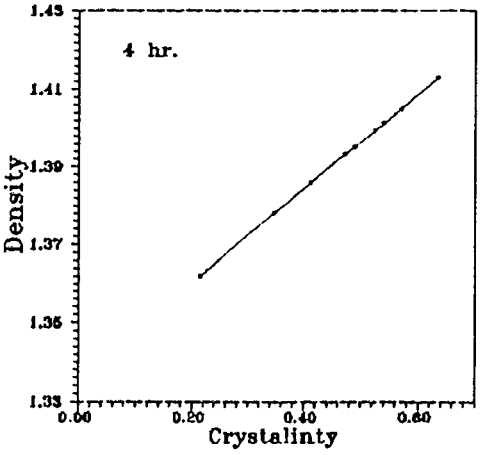

Figure (4-c)

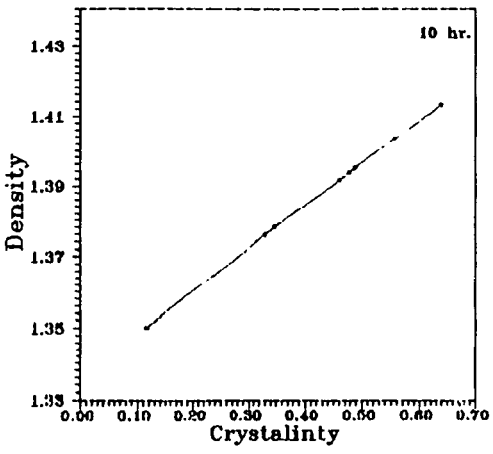

Figure(4-f)

Figure 4 (a–f) Relation between crystallinity and density of polyester fiber at different times (1, 2, 4, 5, 7, and 10 h).

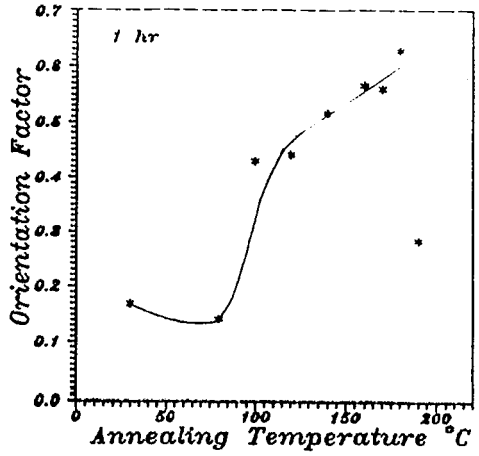

Figure (5-a)

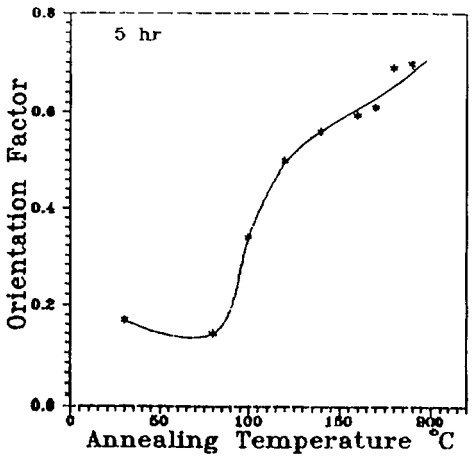

Figure (5-d)

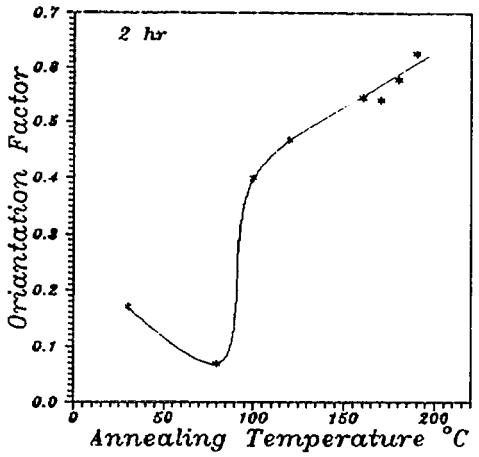

Figure (5-b)

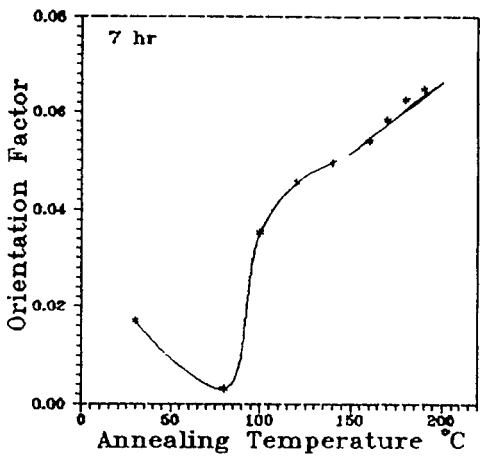

Figure (5-e)

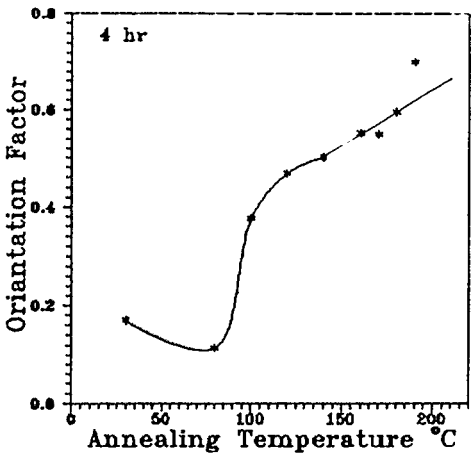

Figure (5-c)

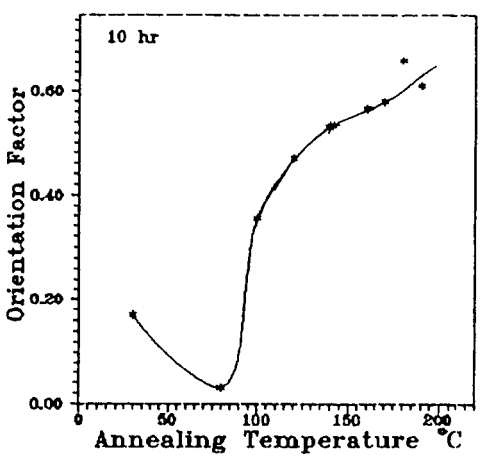

Figure (5-f)

Figure 5 (a–f) Relation between the optical orientation function (f_θ) and annealed temperature at different times (1, 2, 4, 5, 7, and 10 h).

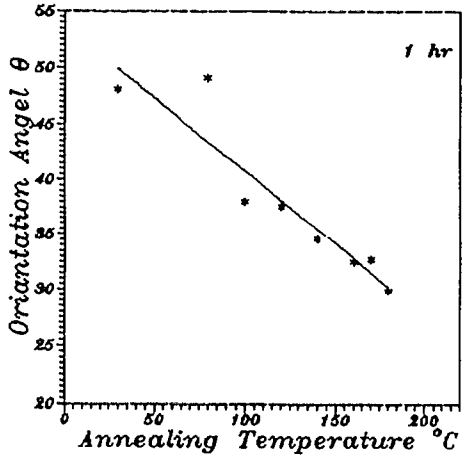

Figure (6-a)

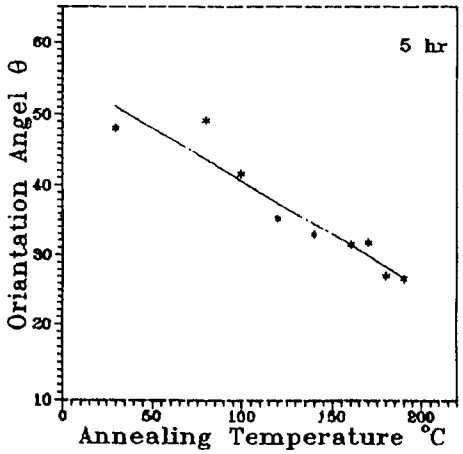

Figure (6-d)

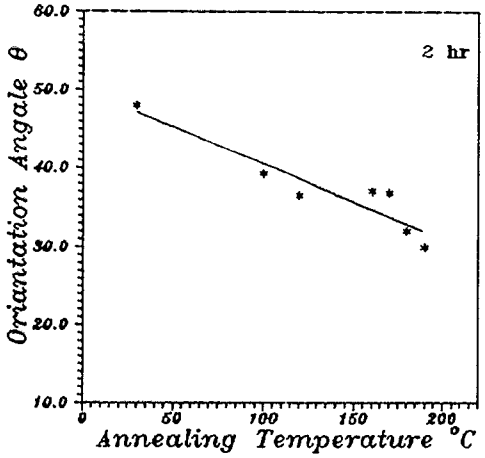

Figure (6-b)

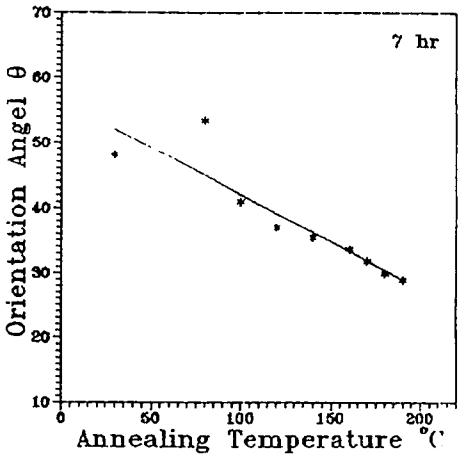

Figure (6-e)

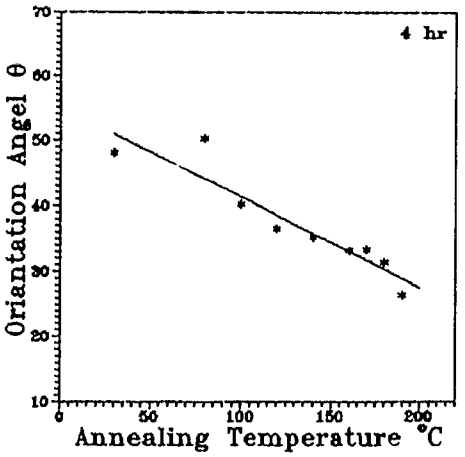

Figure (6-c)

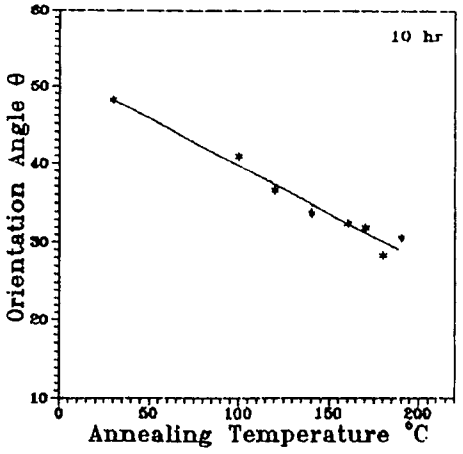

Figure (6-f)

Figure 6 (a–f) The angle of orientation as a function of annealed temperature at different times (1, 2, 4, 5, 7, and 10 h).

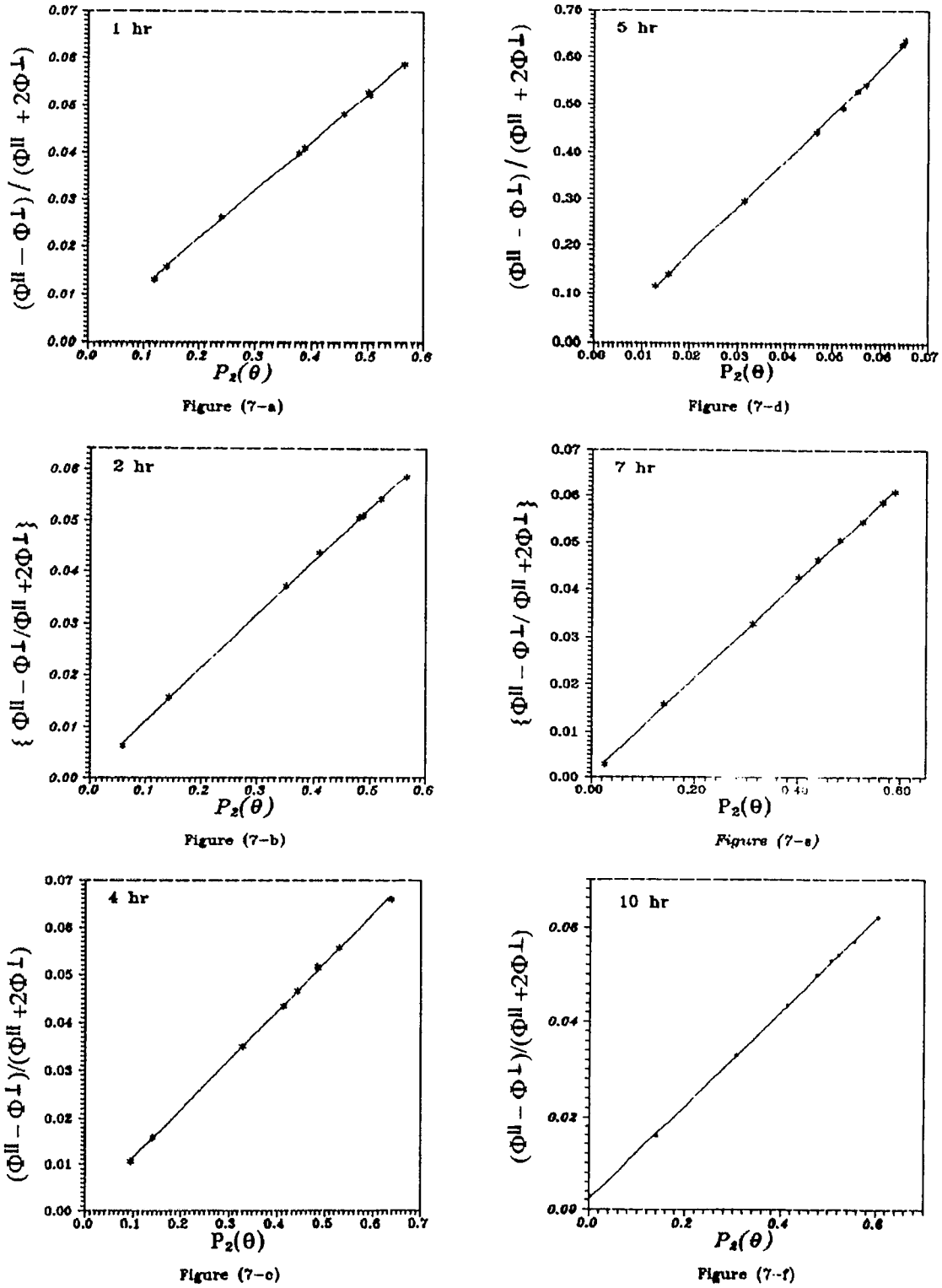

Figure 7 (a–f) Relation between the optical orientation function $\langle P_2(\theta)\rangle$ and the value $\{\Phi^{\parallel} - \Phi^{\perp}/\Phi^{\parallel} + 2\Phi^{\perp}\}$ of annealed PET fibers at different times (1, 2, 4, 5, 7, and 10 h).

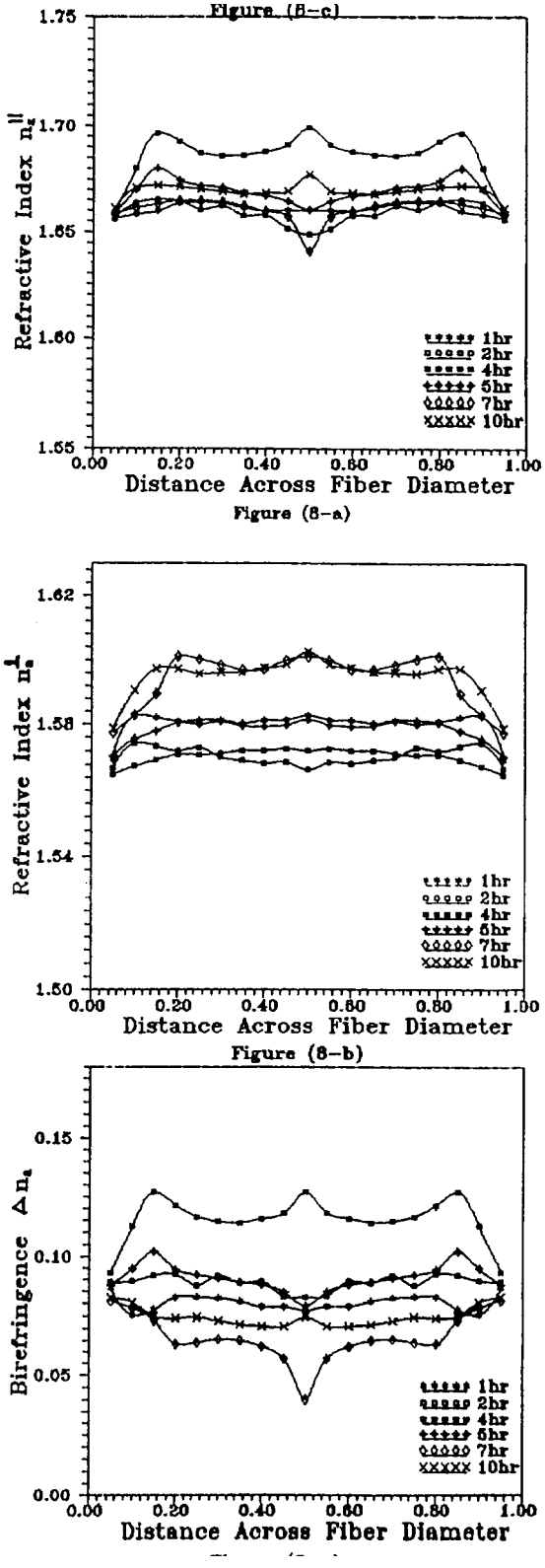

Figure 8 The refractive index profile of polyester fibers with annealing times: (a) $n^{\parallel}$; (b) $n^{\perp}$; (c) Δn.

been offered for the observed birefringence values, the overall orientation, density, and the degree of crystallinity. The first explanation is about the observed decrease in the birefringence values at the beginning of annealing[38]; this means a decrease in the overall orientation as seen from Figures 2 and 5. This could be explained due to the entropy driven to recoil the chains. Therefore, at the beginning of the annealing process, the chains use the thermal energy for recoiling, and shrinkage may occur accompanied by a decrease in the orientation. As crystallization begins, chains are anchored in the crystals and long-range motion and further shrinkage are hindered.[39] So, the overall orientation increases with increasing annealing temperatures and time by further crystallization along the fiber axis of the already oriented crystals. The second explanation is the suggestion concerning the importance of the free-volume effect. When the inner part of a long polymer chain is surrounded by some of the crystallites, then, at suitable annealing conditions, the outer short part of that long chain starts folding in order to construct a new crystallite. Following this, the folded part slowly pulls out the inner part and a new crystallite is formed, leaving a large free volume[43] enclosed between several crystalline regions. Provided that the annealing conditions for this process are sufficient to produce shrinkage of the whole system, the majority of the crystallites will approach each other, enclosing a large closed free volume between them. This mechanism provides an explanation of the variations of density, crystallinity, and birefringence and the importance of the free-volume effect for PET.

CONCLUSION

From the measurements and calculations relating the change of optical properties due to the thermal annealing process for polyester fibers, the following conclusions may be drawn:

1. The microinterferograms clearly identify differences in optical path variations due to different annealing conditions.
2. As $n_a^{\parallel}$ increases, the process of axial orientation increases crystallinity by both orienting the molecules and bringing them closer together, enabling crystallites to form from formally amorphous regions.
3. Annealing the fibrous structure, however, affects the diffusion properties.
4. The effects of the annealing process shows

that the final apparent mass crystallinity achieved for polyester fibers depends on the annealing time and temperature.

5. Changes in n_{iso} with annealing time indicate a change in the specific volume of polyester fibers on annealing, which is clear from Table I.
6. The annealing process affects other physical properties (mechanical, thermal, electrical, elastic, etc.) of the polyester as well as its optical properties. Further studies should be carried out in order to detect which properties are improved by annealing.
7. Evaluation of the crystallinity with the annealing temperature shows a decrease at first annealing temperatures (80°C) in all times of annealing, which means a recoiling of the chains. This is attributed to the entropy driven due to recoiling of chain units of polyester fiber during the beginning of the annealing process.
8. Study of the density variations due to annealing indicates the mass redistribution associated with the annealing process of polyester fibers. These changes are indicative that the transformations had occurred.
9. As the annealing temperature increases, the orientation angle decreases (Fig. 6).
10. It is found that increasing annealing temperature and time gives an increase in the optical orientation function (Fig. 5), while the value $(\Delta\alpha/3\alpha_0)$ which depends upon the molecular structure remains constant.
11. Thermal annealing can provide supplementary information on the structural features related to the thermal performance of materials, where the variation of specific volume is related to crystallinity, density, and mass redistribution of the sample.
12. The refractive index profile of PET fiber at different annealing times throws light on the changes in orientation of the molecules along the fiber axis.
13. The results shown in Table II indicate that the constant K varies with different annealing conditions.

In conclusion, the structural orientation changes due to the annealing process as observed by both two-beam and acoustic techniques is very promising and further study is required in areas which have not yet been explored. Since $n_a^{\parallel}$, $n_a^{\perp}$, Δn_a, n_{iso}, and P_{iso} are a consequence of the material annealed, so reorientation of PET fibers may occur not only during fabrication but also after the fabrication process.

REFERENCES

1. M. A. Neil, R. A. Duckett, and I. M. Ward, *Polymer,* **29,** 54 (1988).
2. R. J. Samuels, *J. Polym. Sci. Part A2* 781–785 (1972).
3. J. Purvis, D. I. Bower, and I. M. Ward, *Polymer,* **14,** 398 (1973).
4. M. Kashiwagi, A. Cunningham, A. J. Manual, and I. M. Ward, *Polymer,* **14,** 11 (1973).
5. J. H. Nobbs, D. I. Bower, I. M. Ward, and D. Pastterson, *Polymer,* **15,** 28 (1974).
6. J. H. Nobbs, D. I. Bower, and I. M. Ward, *Polymer,* **17,** 2 (1976).
7. J. H. Nobbs, D. I. Bower, and I. M. Ward, *Polymer,* **19,** 1100 (1978).
8. J. M. Perena, R. A. Duckett, and I. M. Ward, *J. Appl. Polym. Sci.,* **25,** 1381 (1980).
9. D. I. Bower and I. M. Ward, *Polymer,* **23,** 645 (1982).
10. A. A. Hamza, I. M. Fouda, T. Z. N. Sokkar, M. M. Shahin, and E. A. Seisa, *Polym. Test.,* **11,** 297 (1992).
11. I. M. Fouda and M. M. El-Tonsy, *J. Mater. Sci.,* **25,** 121 (1990).
12. J. R. Samuels, *Structured Polymer Properties,* Wiley, New York, 1974, pp. 20, 51, 63, 219.
13. P. Polukhin, S. Gorelik, and V. Vortontsov, *Physical Principle of Plastic Deformation,* Mir, Moscow, 1983, p. 275.
14. M. Pluta, *J. Microsc.,* **96,** 309 (1972).
15. M. Pluta, *J. Opt. Acta,* **18,** 661 (1971).
16. A. A. Hamza, *Text. Res. J.,* **50,** 731 (1980).
17. J. R. Samuels, *Structured Polymer Properties,* Wiley, New York, 1974, pp. 50–60.
18. I. M. Ward, *Structure and Properties of Oriented Polymers,* Applied Science, London, 1975, p. 57.
19. S. R. Padibjo and I. M. Ward, *Polymer,* **24,** 1103 (1983).
20. H. Hannes, *Z. Kolloidz Polym.,* **250,** 765 (1972).
21. P. H. Hermans, *Contribution to the Physics of Cellulose Fibers,* North-Holland, Amsterdam, 1946.
22. H. de Vries, *Colloid Z. Polym. Sci.,* **257,** 226 (1979).
23. I. M. Ward, *Proc. Phys. Soc. Lond.,* **80,** 1176 (1962).
24. I. M. Ward, *J. Polym. Sci. Polym. Symp.,* **53,** 9 (1977).
25. A. Cunningham, G. R. Davies, and I. M. Ward, *Polymer,* **15,** 743 (1974).
26. R. S. Stein and G. L. Wilkes, *Structure and Properties of Oriented Polymer,* I. M. Ward, Ed., Applied Science, London, 1975, p. 57.
27. P. H. Hermans and P. Platzek, *Kolloid Z.,* **88,** 68 (1939).
28. O. Kratky, *Kolloid Z.,* **64,** 213 (1933).

29. I. M. Fouda, M. M. El-Tonsy, and M. M. Shaban, *J. Mater. Sci.,* **26,** 5085 (1990).
30. M. M. El-Tonsy, A. M. Shaban, and I. M. Fouda, *Polym. Bull.,* **25,** 507 (1991).
31. A. A. Hamza, I. M. Fouda, M. M. El-Tonsy, and F. M. EL-Sharkawy, *J. Appl. Polym. Sci.,* **56,** 1355 (1995).
32. N. Subrahmanyam and B. Lal, *A Text Book of Sound,* 2nd ed., Vikas, New Delhi, 1979, p. 143.
33. G. Le Bourvellee and J. Beautemps, *J. Appl. Polym. Sci.,* **39,** 329 (1990).
34. G. Le Bourvellec, L. Monnerie, and J. P. Jarry, *Polymer,* **28,** 1712 (1987).
35. B. Wunderlich, *Macromolecular Physics,* Academic Press, New York, 1973, Vol. 1.
36. A. A. Hamza, T. Z. N. Sokkar, and M. M. Shahin, *J. Appl. Phys.,* **70,** 4480 (1990).
37. A. A. Hamza, I. M. Fouda, M. M. El-Tonsy, and F. M. El-Sharkawy, *J. Appl. Polym. Sci.,* **60,** 1239 (1995).
38. D. J. Williams, *Polymer Science and Engineering,* Prentice-Hall, Englewood Cliffs, NJ, 1971, Chap. 7, p. 197.
39. P. N. Peszkin and J. M. Schultz, *J. Polym. Sci. Part B Polym. Phys.,* **24,** 259 (1986).
40. M. F. Vallat and D. J. Plazck, *J. Polym. Sci. Part B Polym. Phys.,* **26,** 556 (1988).
41. A. Z. Zachariodes and S. R. Porter, *The Strength and Stiffness of Polymers,* Marcel Dekker, New York, Basel, 1983, p. 121.
42. D. C. Bassett, *Principles of Polymer Morphology,* Cambridge University Press, Cambridge, 1981, p. 124.
43. N. Brown and I. M. Ward, *J. Polym. Sci. A-2,* **6,** 607 (1968).